nzsee
NEW ZEALAND SOCIETY FOR EARTHQUAKE ENGINEERING

Seismic response of frames with building cladding elements

J. B. Robertson

Aurecon, Auckland, New Zealand

W. S. Edwards

Downer Group, Christchurch, New Zealand

Z. Luo

Xi'an University of Architecture and Technology, Xi'an, China

G. A. MacRae

University of Canterbury, Christchurch, New Zealand

ABSTRACT

This paper presents the concept, methodology and findings of the analysis of frames with building cladding elements exposed to seismic events. Inelastic nonlinear push-pull analyses, and hand analyses are conducted to verify the consistency between the two types of analysis and to demonstrate the cladding self-centring effect. The effect of mass ratio, between the frame and cladding, is then investigated. Inelastic time history analyses with a suite of records are conducted to evaluate the dynamic effect of the different weight cladding elements on the structure in terms of maximum and residual displacement both ignoring and considering *P*-delta effects.

It was found that the cladding elements caused an increase in frame initial stiffness and lateral strength, and this was modelled consistently with hand, and numerical, pushover analyses. These parameters increased as more weight was placed on the cladding elements. Also, during the inelastic time history analyses, it was demonstrated that both building peak and residual displacements decreased, both ignoring and considering P-delta effects. This is consistent with analyses of bilinear oscillators which also show similar trends with change in hysteresis loop. Using the methods described, it is possible to generate the hysteresis curves for evaluation of the likely changes in peak and residual displacements in design.

1 INTRODUCTION

The February 2011 Christchurch earthquakes had a large economic impact on New Zealand. Such earthquakes can impose high demands on buildings resulting in significant damage. Historically, building vertical non-skeletal elements (NSEs), such as precast concrete panels (PCPs), glazed curtain walls (GCWs), and internal partition walls (IPWs), are not assumed to be part of the structural skeleton of the building. Instead, they have generally been considered only as adding mass, without any other structural influence. For such vertical NSEs to not be damaged during large frame horizontal deformations, they can be designed to rock. As they rock, the lateral strength of the structure is increased and there is also a recentering tendency. These effects on structural performance are not generally considered in design and may improve structural performance and reduce the tendency for frame cumulative inelastic displacements in one direction.

For engineers to design structures to perform well, and to avoid unnecessary conservatism, there is a need to ensure that elements, including rocking vertical NSEs, affecting structural performance are considered.

This paper seeks to address this need by seeking answers to the following questions:

1. How do rocking vertical NSEs (represented as rocking cladding elements in this paper) affect the hysteretic performance of structures?
2. Can their effect be modelled?
3. What is their effect on peak and residual displacements of a simple structure?
4. What are the implications of the findings?

2 LITERATURE

Many structures, including moment-resisting frames (MRF) and buckling restrained braced frames (BRBF) produce bilinear hysteresis loops when subject to cyclic lateral loading as shown in Figure 1a. If these structures have a low post-elastic stiffness, and are also subject to *P*-delta effects, they may have a negative post-elastic stiffness resulting in dynamic instability as shown in Figure 1b. This may cause a frame to experience seismic ratcheting (i.e., cumulative yielding of a structure in one horizontal direction) during earthquake shaking (MacRae, 1994, MacRae et al., 2022).

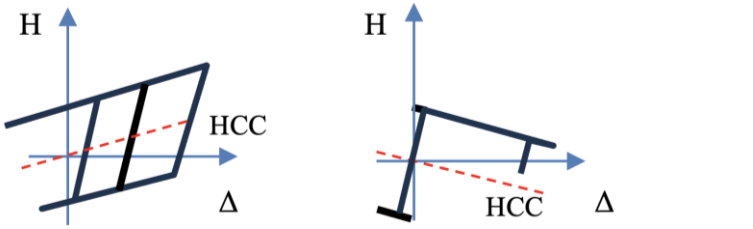

(a) Dynamically Stable *(b) Dynamically Unstable (P-delta)*

Figure 1. Dynamic stability (MacRae 1994).

For a single storey structure with a lumped mass at the top, the *P*-delta effect reduces the stiffness, *k*, by *P*/*L* as shown in Equation 1 (MacRae, 1994), where *P* is the axial force (=*mg*), *L* is the height to the centre of mass, *m*, and *g* is the acceleration of gravity.

$$k_p = k - P/L \tag{1}$$

The vertical NSEs, such as cladding elements attached to the exterior of a frame, may be designed (i) without any consideration for earthquake, in which case damage is possible within the frame, (ii) to slide, which can prevent damage during shaking in the direction of the frame supporting the NSE, but can result in damage as the NSEs interact at the corners during bi-directional shaking, or to rock as shown in Figure 2. Here, vertical slots in the vertical NSE, with bolts fixed in position to the frame, allow vertical sliding as shown in Figure 3. As the frame moves over, the cladding rocks due to the floor's relative horizontal deformations. Due to this rocking, uplift occurs on one side of the panel relative to the frame. The panel self-weight causes a restoring force and recentering tendency which tends to mitigate seismic ratcheting. Furthermore, as panels deform with respect to each other, sealant between the panels deforms, increasing the restoring forces. However, Bhatta et al. (2022) indicate that such forces are usually negligible. Arifin (2017) considered the change in period of a building with and without cladding and found that the cladding increased or decreased the period, by less than 1% and their presence generally decreased seismic drifts.

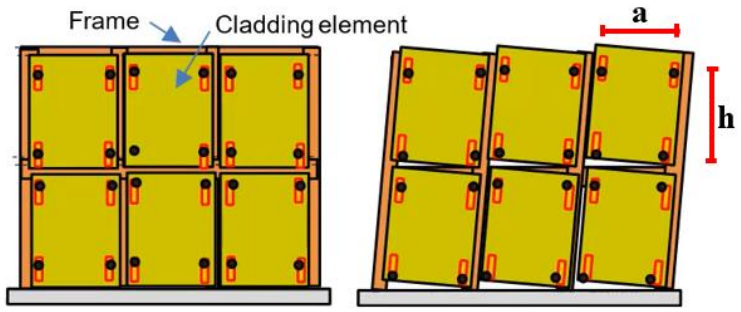

(a) At rest *(b) At peak displacement*

Figure 2. Rocking vertical NSE behaviour (MacRae 2019)

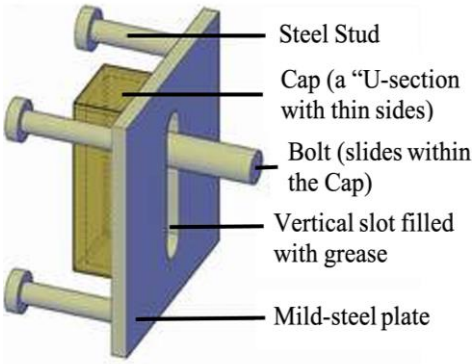

Figure 3. Panel connections (Bhatta et al. 2022).

3 CLADDING CONSIDERATIONS

Cladding can be supported on structures in different ways. A rectangular cladding panel supported vertically at the top, such as that shown in Figure 4, will uplift when the panel lateral force, H, multiplied by the vertical distance between the panel supports (mm), h, is greater than a function of the panel weight, W, multiplied by the horizontal distance between the panel supports (mm), $a/2$, from moment equilibrium about Point A. This can be rearranged to give the uplift force H_{uplift} as $Wa/(2h)$. This is this first term on the RHS of Equation 2.

As pushing continues, the displacement Δ increases and this results in an additional force, H'. This effect of the deformation related forces is shown in Figure 5 where the panel is treated as a deforming rod. By taking moments about the top support, $H'h = W\Delta_1$, where Δ_1 is the displacement of the centre of mass, h_1 is vertical distance from the point of rotation to the centre of mass, H' is the lateral force due to deformations. Here H' is equal to $W\Delta_1/h = W\Delta h_1/h^2$ as shown in Equation 2, since $\Delta_1 = \Delta h_1/h$. The cladding lateral force, H, is given by Equation 2. The second term may be relatively small because $\Delta h_1/h$ is generally much less than $a/2$.

$$H = H_{uplift} + \Delta H = \frac{Wa}{2h} + \frac{W\Delta h_1}{h^2} \quad (2)$$

It is noted that when computer analyses are conducted the $W\Delta/h$ term is only captured when second order effects are modelled.

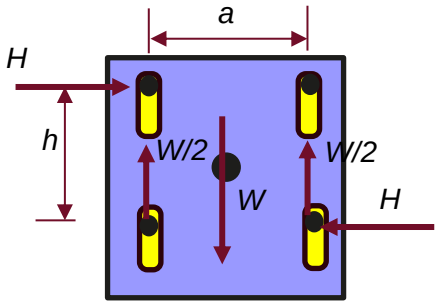

(a) Before Uplift

Figure 4. Uplift Mechanism

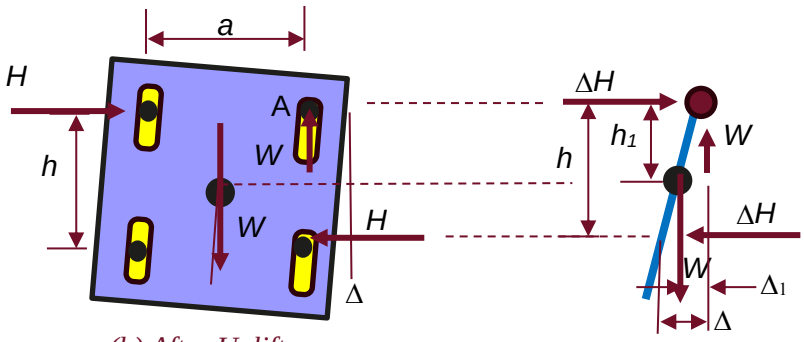

(b) After Uplift

Figure 5. Post uplift forces

If the cladding panel gravity force is carried on the lower support, then the second term in Equation 2 becomes negative indicating a decrease in H with increased displacement, because the panel becomes less stable. It therefore seems desirable to support the panel on the upper beam in general. In many actual cladding support situations, the cladding supports shown within the structure are only required to resist horizontal force (in-plane and out-of-plane), with additional larger vertical supports provided near the base of each panel. This will also tend to cause a negative post-elastic stiffness, although this effect may not be large. It is also noted that lateral in-plane restraint is generally applied at one top support and one bottom support in each panel to prevent the effects of the panel binding causing an unpredictable strength increase, as in-plane drift occurs.

When a storey has n cladding panels, instead of one panel the same width of frame, a, then while W is the total weight of all panels, then H is given as is Equation 3, and is lower than for one panel.

$$H = \frac{n.(W/n).(a/n)}{2h} + \frac{W\Delta h_1}{h^2}$$

$$= \frac{Wa/n}{2h} + \frac{W\Delta h_1}{h^2} \quad (3)$$

When cladding is placed on a single storey frame with elastoplastic characteristics, the total force resistance is that from (i) the frame alone (in Figure 6a), plus that from (ii) the rocking cladding alone as shown in Figure 6b where the frame is pinned. It may be seen that the stiffness of the system is high before uplift of the panel occurs on one side. This initial stiffness is not infinite, but it depends on the stiffness of the other frame members, and cladding connections. The increase in lateral force from the cladding with displacement is small enough to not be shown. The total resistance is given by the black line in Figure 6c. The cladding resists rocking until the uplift force, H_{uplift}, is attained. Modelling cladding weight explicitly increases the lateral force resistance and recentring tendency, but it also increases the building stiffness and decreases the building period, and likely total displacements.

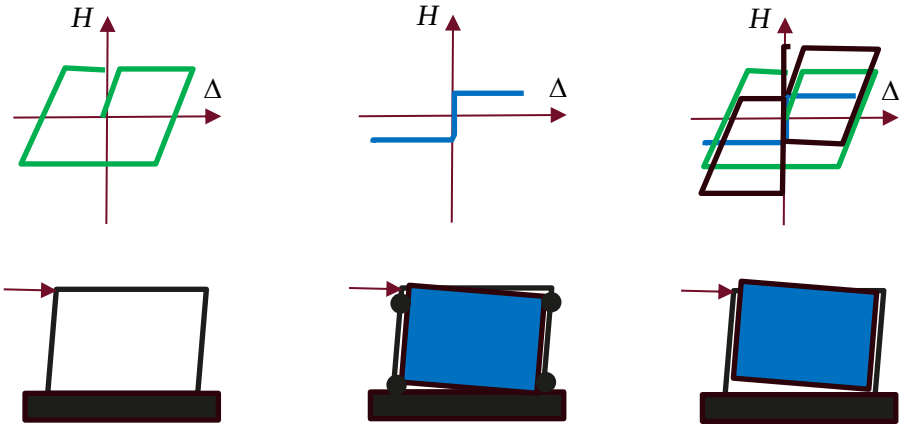

(a) EPP MRF *(b) Rocking Cladding* *(c) Combined*

Figure 6. Idealised Hysteresis Loops for the Frame, Cladding, and System

4 METHODOLOGY

An initial hand analysis of a simple single-bay, single-storey moment resisting frame (MRF) with fixed base and top connections, similar to that in Figure 3c, was used. The height to the centre of the beam centreline, *L*, is 2.605 m and distance between column centrelines is 2 m. It is assumed that the beam is stiff so Equation 4 approximates the MRF lateral stiffness, *k* (kN/mm), by considering it to be two fixed end 100mm × 100mm × 10mm square hollow box section columns with a second moment of inertia, *I*, equal to 4,620,000 mm^4 where, *E* is the elastic modulus of steel of 200 GPa.

$$k = \frac{24EI}{L^3} \tag{4}$$

Frame mass, *m*, of 7900 kg, was selected to obtain a fundamental period, *T* (= $2\pi\sqrt{(m/k)}$), of 1.0s. The frame strength was selected by controlling the elastic-perfectly plastic fibre section hinge strength at the column ends to give a yield drift of 0.9%. The frame vertical gravity force, *P*, is *mg* = 77.2 kN.

The vertical NSE cladding panels contained four slotted holes into which round rods are fitted. These rods can move vertically in the holes as shown in Figure 3, and the ends of the rods within the slotted holes prevent the panels from moving away from the building surface. The other ends of these rods are fitted to fixed support locations relative to the beams. In the model, the four cladding supports are connected to the frame with stiff link elements. Cladding had supports spaced 1800 mm horizontally, *a*, and 2400 mm vertically, *h*, with the frame centreline dimensions. At their rest position, they were placed symmetrically about the centre of the panel. The cladding is supported vertically from the top nodes. Panel rocking occurs as the connector rods, connected to the frame, slide vertically in the panel. Sliding is restricted in each hole in the horizontal direction. No sliding friction is assumed and any effect of the sealant stiffness is ignored. Once the rods have slid to the end of their hole, sliding is restricted.

The ratio of cladding weight to total storey weight, considered in the push-pull analysis, were 5%, 25%, and 50%. For inelastic time history analysis, they were 0%, 5%, 10%, 20%, 30%, 40%, and 50%. The total weight of the frame model, including the cladding, was 77.2 kN in every case. For example, the weight ratio of 5% included a cladding weight of 3.9 kN and a frame weight of 73.3 kN. The weight ratio of 50% is equivalent to having all of the story weight in the cladding for a building of square plan with cladding all the way around. While this is obviously unrealistic, it provides a bound on the cladding weight ratio. For a typical rectangular building with heavy cladding, it is unlikely that the cladding weight ratio considering all vertical rocking would exceed 5%, and it is likely significantly lower than this.

Modelling and analysis was performed using the STKO graphical user interface (GUI) with OpenSEES. Consideration of the response with and without *P*-delta effects was conducted.

Pushover analysis was conducted by hand. Also, push-pull analysis was conducted to drifts of 1% (26 mm), 2.5% (65 mm), and 5% (130 mm) using a displacement control integrator.

For the time history analysis an initial stiffness proportional Rayleigh model, with 5% damping at periods of 1.0s and 0.047s, was used. The 22 ground acceleration histories from the ATC-63 far-field ground motion set were scaled to cause a lateral force reduction factor, *R*, equal to 4.0 (which is equivalent to k_μ/S_p in NZS1170.5). The Newmark integrator with an adaptive time step is used. Batching, to run multiple analyses and extract the key information, was conducted using a Python script and PowerShell.

5 BEHAVIOUR

5.1 Hand Analysis

Using the simple calculations shown in Equation 4, the lateral force required to displace the moment resisting frame laterally by 24.3 mm (yield displacement) was calculated as 7.85 kN without considering the *P*-delta effect.

5.2 Push-Pull

Figure 7a confirms the hand analysis which had a lateral force of 7.68 kN without considering *P*-delta. The *P*-delta effect, in Figure 7b, for this particular short frame is significant, and extrapolation of the top line indicates that “static instability” is likely to occur at a displacement of about 250 mm. After this displacement, the structure will tend to collapse.

Figure 8, which gives the push-pull analyses of the system with different cladding weight ratios at different drift levels, indicates that:

a) there is a greater initial stiffness, which is associated with a lower frame period, and lower total displacement demands,
b) the strength increases significantly (from 7.8 kN up to 23 kN) as a result of a greater proportion of mass being placed in the cladding. This additional force reduces the ratchetting tendency, but it needs to be carried by the frame elements.
c) there is increased dynamic stability. The hysteresis loop shape is simply that of the MRF offset by the rocking cladding strength in the positive and negative displacement directions respectively as per

Figure 6c. This increases the frame hysteresis dynamic stability as shown in Figure 1 so the ratchetting tendency is likely to be decreased. This, together with the previous two points, indicates that expected displacement demands.

d) The rocking increase in strength with displacement, as indicated by the second term in Equation 2, is low as shown by the curves being almost flat.

e) At 1% drift there was very little MRF yielding, as shown in Figure 7a and 8a, but this increases with greater displacements as shown in Figures 8b and 8c.

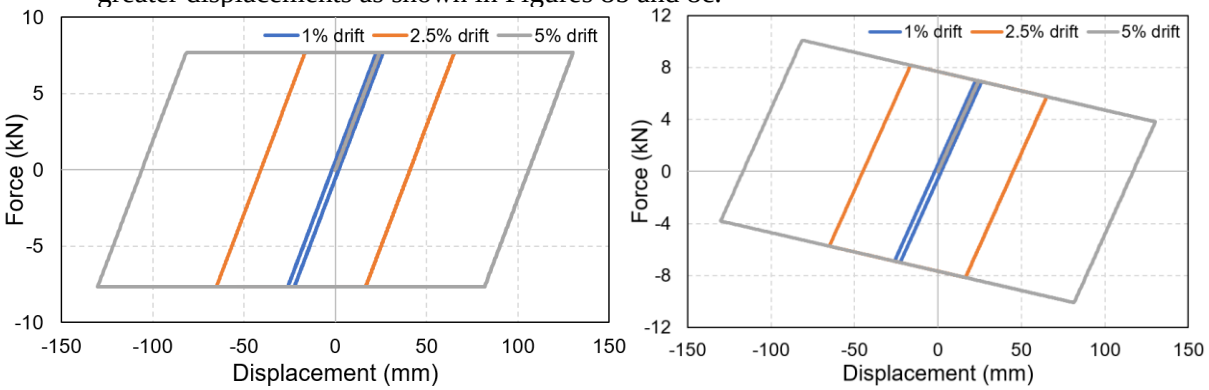

(a) with P-delta effects ***(b) with P-delta effects***

Figure 7. MRF Hysteresis Loops at different drifts (No cladding)

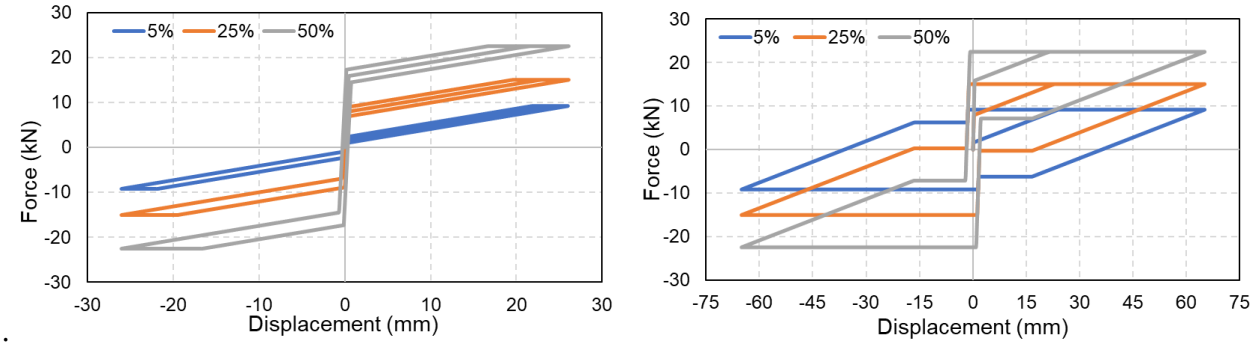

(a) 1% drift *(b) 2.5% drift*

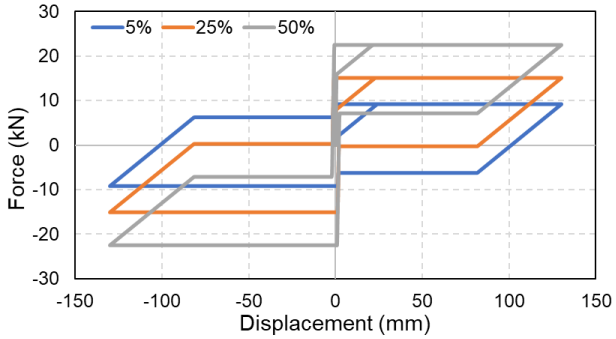

(c) 5% drift

Figure 8. Frame hysteresis loops for different cladding weight ratios (No P-delta)

Table 1, which summarises the push-pull numerical behaviour, and shows that the total system forces obtained from the analytical (hand analysis) method, and the numerical method, at 5% frame drift agree well. The

difference may be due to the numerical bolt modelling where a small force is required to initiate sliding. The hand analysis used Equation 2 and both the cladding (VNSE), and MRF effects, sum up to the obtain the total strength.

Table 1. Push-Pull Analyses Summary when ignoring P-delta (Drift =5%)

Weight Ratio	Analytical			Numerical
	VNSE's (kN)	MRF (kN)	System (kN)	System (kN)
5%	1.45	7.85	9.3	9.9
25%	7.24	7.85	15.1	15.8
50%	14.48	7.85	22.3	23.3

When the *P*-delta effect is considered in the push-pull analyses, the hysteresis loop stiffness is reduced by P/L, where L is the storey height, as shown in Figure 9.

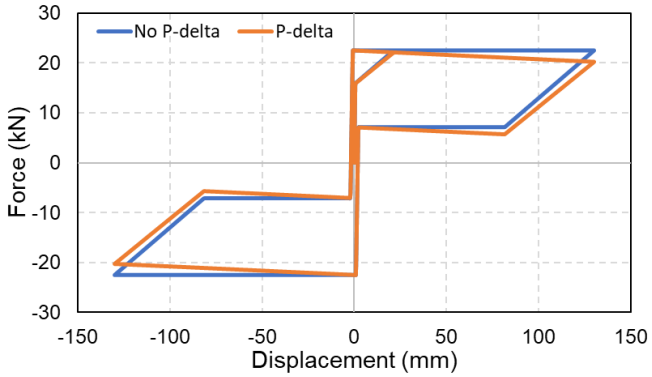

Figure 9. Effect of P-delta on Push-Pull Analysis 5% drift (50% Cladding Weight Ratio)

The effect of *P*-delta at 5% drift, which is shown in Table 2, indicates lower forces when compared to Table 1, as expected. The change in force is $W\Delta h_1/h^2 - P\Delta/L$ (from the second term in Equation 2 and MacRae (1994)). Here, in the model, the centre of panel weight was assumed to be at the bottom support level, so $h_1 = h$ in Figure 5, and storey height of the frame was assumed to be equal to the vertical distance between panel supports, h, (i.e. $h = L$), then the change in force is $W\Delta/h - P\Delta/h$. For example, for a cladding weight ratio, *CWR*, of 25% (i.e. $W = CWR = 0.25P$) at an interstorey drift ratio (ISD), of 5% (i.e. $\Delta = ISD.h = 0.05h$), since the force change is $W\Delta/h - P\Delta/L = P.ISD.h.(CWR/h - 1/h) = P.ISD.(CWR - 1)$ = 77.2 kN x 0.05 x (0.25 - 1) = 3.0mm. This is consistent with the numerical results of 15.8 - 12.8 = 3mm from Tables 1 and 2. Here, the cladding effect compensates for 25% of the *P*-delta effect. This ratio depends on the *CWR*. [In general, it would be better for the model place the centre of weight at the centre of the panel, to consider the actual difference between h_1 and h, and to consider that the storey height, L, may be different from the distance between panel supports, h.]

Table 2. Push-Pull Analysis Summary with P-delta (Drift =5%)

Weight Ratio	Analytical			Numerical
	VNSE's (kN)	MRF (kN)	System (kN)	System (kN)
5%	1.66	4.53	6.19	6.3
25%	8.29	4.53	12.82	12.8
50%	16.57	4.53	21.1	21.0

5.3 Inelastic Time History Analysis

Figure 10a shows that a greater cladding weight ratio significantly decreases both peak drifts when there is no *P*-delta effect. The residual drifts shown in Figure 10b reduced more rapidly, going to zero when CWR is 10%.

The static instability displacement can be found for the structures subject to *P*-delta, where there is a negative post-elastic stiffness. It occurs when the loading strength drops to zero. Extrapolation from Figure 7b shows that when there is no cladding effect, this displacement is approximately 260mm as shown in Figure 10. This displacement increases with increasing strength caused by the cladding effect.

The *P*-delta effect is quite severe for the scenario considered. It caused collapse (i.e. displacements exceeding the static instability displacement and not returning to lower displacements) for *CWR* less than 30%. It is clear that increasing the *CWR* can mitigate the possibility of collapse.

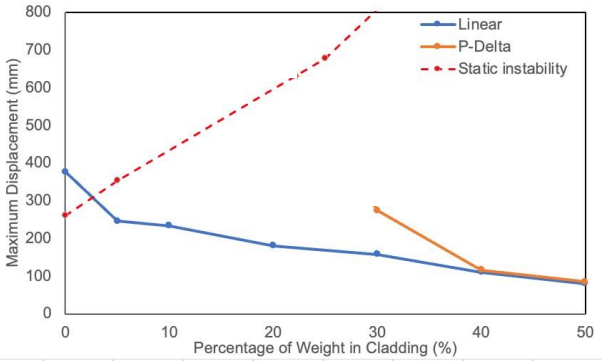

(a) Maximum Displacement

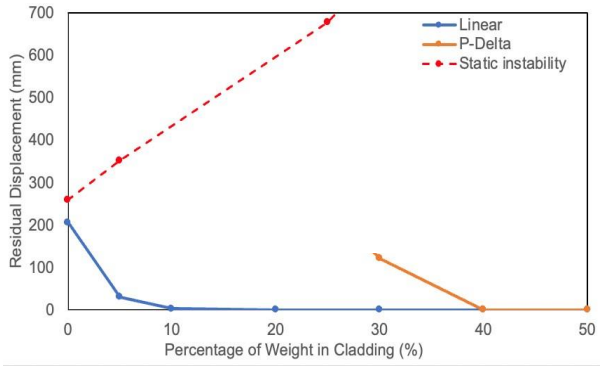

(b) Residual Displacement

Figure 10. Displacements vs Cladding Weight Ratio

It is also interesting that the cases with and without P-delta converge to the same peak displacement value for *CWR* > 40%. This may be because the structure tends towards being elastic with a very short period and high strength. For these structures, the rocking panels cause zero permanent displacement.

6 CONCLUSIONS

A study was conducted to evaluate the effect of rocking vertical non-skeletal elements (NSEs) on the seismic response of moment-resisting frame structures. It was shown that:

1. Considering explicitly these rocking vertical NSEs increases the lateral stiffness, strength and dynamic stability of structures.
2. This performance can be modelled both by numerical, and analytical (i.e., hand methods), methods, and both approaches give consistent results.
3. Inelastic dynamic time history analysis indicated that as the weight in the cladding increased, the peak and residual displacements decreased. This is consistent with understanding from dynamic stability concepts.
4. The work validates the concept that rocking vertical NSEs may be used effectively to enhance structural performance and this may be considered directly in design.

7 REFERENCES

Arifin, F. (2022). Identification of Cost-Effective Retrofit and/or Rehabilitation Strategies for Steel Buildings, *Masters Thesis, Department of Civil and Natural Resources Engineering, University of Canterbury*. Supervised by Sullivan T. and MacRae G. A. Page 84 Tables 4.13 through 4.15.

Bhatta, J., Dhakal, R. P., Sullivan, T. J., and Lanyon, M. (2022). "Low-Damage Rocking Precast Concrete Cladding Panels: Design Approach and Experimental Validation." *Journal of Earthquake Engineering*, 26(9), 4387-4420.

Dhakal, R. P. (2016). "Seismic performance of non-structural components and contents in buildings." *Earthquake Engineering and Engineering Vibration.*

MacRae, G. A. (1994). "P-Δ effects on single-degree-of-freedom structures in earthquakes." *Earthquake Spectra*, 10(3), 539-568.

MacRae, G. A. (2019). "ILEE ROBUST Building Systems", Presentation to Tongji University, Shanghai, 30 August.

MacRae G. A., Zhao X., Jia LJ, Clifton G. C., Dhakal R., Xiang P., Ramhormozian S., Rodgers G., The China-NZ ROBUST Friction Building Shaking Table Testing Overview, 17th World Conference on Earthquake Engineering, Sendai, Japan, September, 2020. Paper 2g-0044 (C000558).

MacRae, G. A., Lee, C-L., and Yeow, T. Z. (2022). *Seismic Ratcheting Considerations, Asian Conference on Earthquake Engineering (ACEE)*, Taipei, Taiwan, 9-11 November.